

Supporting Information

Covalent assembly of ultrathin polymer nanocapsules to mimic a multienzyme-cascade antioxidative system

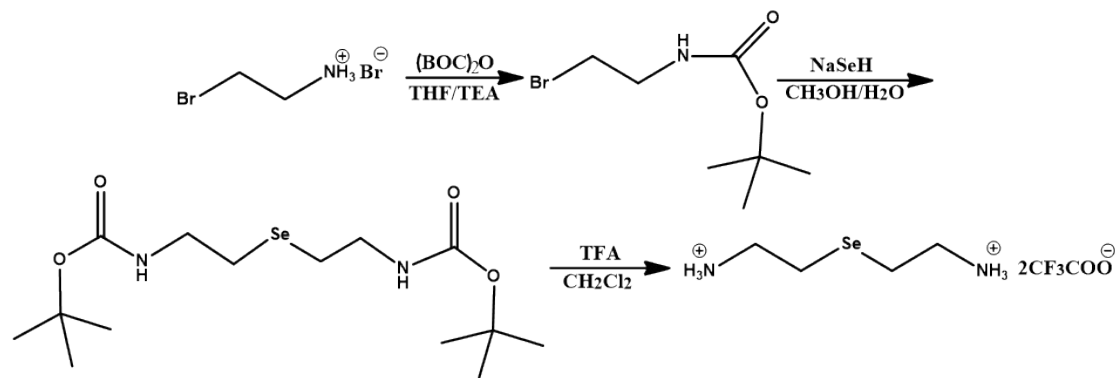
Ruizhen Tian, XiaoTong Fan, Shengda liu, Feihu yang, Quan luo, Chunxi Hou, Jiayun Xu
and Junqiu Liu *

State Key Laboratory of Supramolecular Structure and Materials, College of Chemistry, Jilin
University, 2699 Qianjin Street, Changchun 130012, China, Fax: (+86) 0431-8516845

*Email: junqiuliu@jlu.edu.cn

Experimental Section

1. Synthesis and characterization of target molecules



Scheme S1: The synthetic route of 2,2'-selenobis (ethan-1-aminium).

Synthesis of tert-butyl (2-bromoethyl) carbamate:

2-Bromoethylamine hydrobromide (20.01 g, 0.0976 mol) and tetrahydrofuran (THF, 100 mL) were mixed together, then added 40 mL of triethylamine (TEA). Di-tert-butyl pyrocarbonate (19.17 g, 0.0878 mol) was dissolved in THF (20 mL) and then dropped into the above solution. After the addition was completed, the reaction was continued for 16 hours. After the reaction was over, about 160 mL of solution was evaporated by vacuum, and 100 mL of ethyl acetate was added into the mixture. The mixed solution was washed twice with 0.1 M hydrochloric acid, twice with a saturated sodium chloride solution, then dried over anhydrous sodium sulfate, and finally, the ethyl acetate was evaporated by vacuum to obtain a colorless transparent liquid (15.6 g). ¹H NMR (500 MHz, DMSO) δ 7.10 (s, 1H), 3.44 (dd, J = 11.1, 4.5 Hz, 2H), 3.32 – 3.28 (m, 2H), 1.39 (s, 9H).

Synthesis of 2,2'-selenobis (ethan-1-aminium):

Selenium (1.2 g, 0.015 mol) and Sodium borohydride (0.52g, 0.013mol) were added into a three-necked flask (250 mL), and then the whole system was deoxidized and under the condition of nitrogen atmosphere. In the case of a continuous stream of nitrogen, 10 ml of deoxygenated water was slowly added to the system and a large amount of bubbles appeared. When no bubbles were generated, the tert-butyl (2-bromoethyl) carbamate (8.5 g, 0.038 mol) is dissolved in 20 ml of methanol and deoxygenated, then rapidly added to the above system, heated to 40 ° C and reacted for 20 hours. After cooling to room temperature, methanol was evaporated by vacuum and extracted with ethyl acetate. The crude product obtained was purified by column chromatography. The purified product was dissolved in dichloromethane (50 mL), 2ml of trifluoroacetic acid was added, and the reaction lasted for 5 hours. Then dichloromethane was evaporated by vacuum, 100ml ethyl ether was added to the residue, and the precipitation was filtered and collected, and the white solid powder was obtained by washing with ethyl ether for three times. ¹H NMR (500 MHz, DMSO) δ 8.04 (s, 6H), 3.10 – 3.04 (m, 4H), 2.80 – 2.74 (m, 4H). MS (ESI) = 169. [M-H]⁺

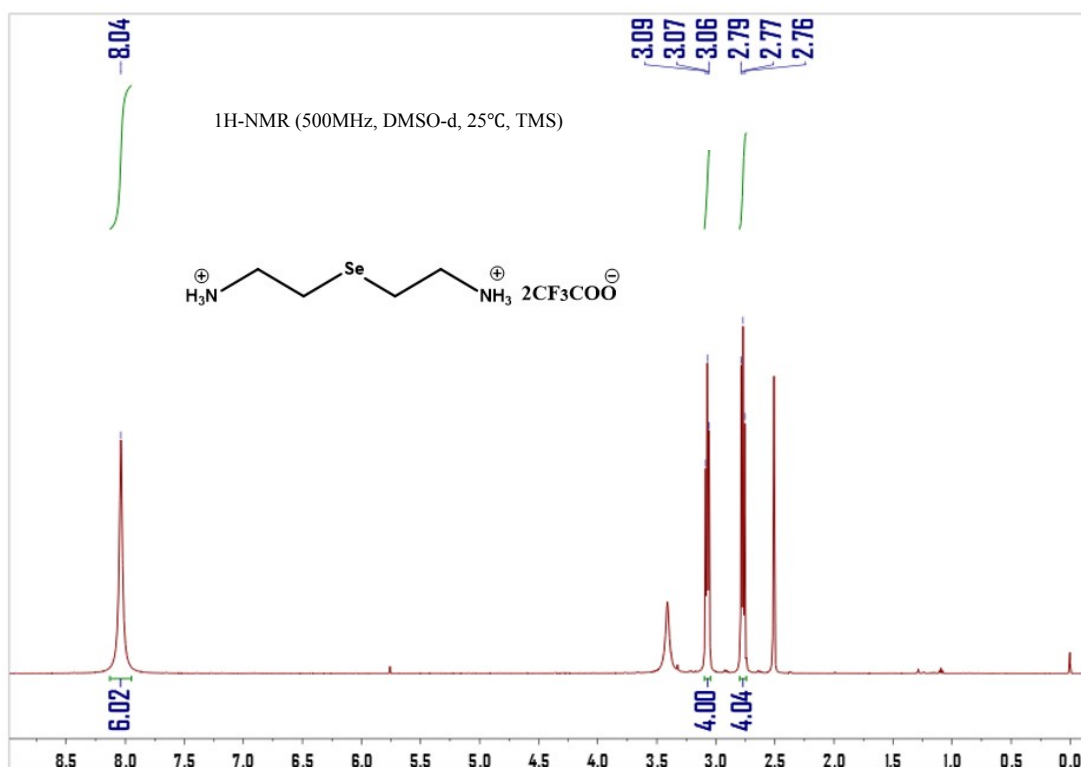


Figure S1: The $^1\text{H-NMR}$ (500MHz, DMSO-d, 25°C, TMS) spectrum of 2,2'-selenobis(ethan-1-aminium).

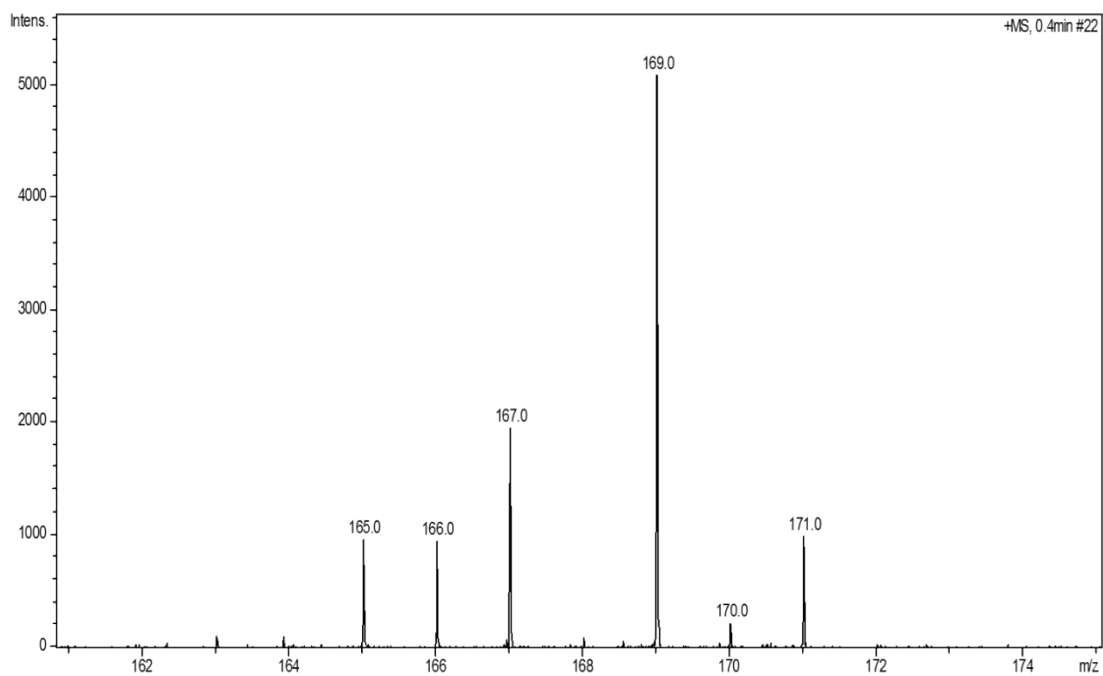
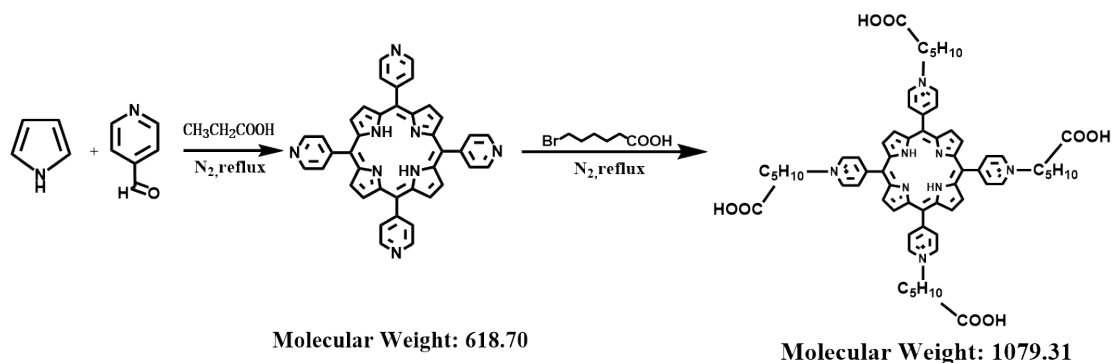


Figure S2: ESI-MS analysis of 2,2'-selenobis(ethan-1-aminium).



Scheme S2: The synthetic route of TPyP and CATPyP.

Synthesis of 5, 10, 15, 20-tetrakis (4'-pyridyl) porphyrin (TPyP):

4-Pyridinecarboxaldehyde (7.32 g, 60 mmol) and 300 mL of propanoic acid were mixed together, then the mixture was heated to reflux under the condition of nitrogen atmosphere, followed by dropwise adding 50 mL of propanoic acid dissolved pyrrole (4.02 g, 60 mmol). The mixture was refluxed for another 2.5 hours under the condition of nitrogen atmosphere. After cooling to room temperature, about 250 mL of propanoic acid was evaporated by vacuum, and 100 mL of methanol was added into the mixture. The resulting precipitate was filtered and washed several times using ethanol, then dried under vacuum to obtain the purple solid (1.9 g, 3.07 mmol, 20.5%). ¹H NMR (500 MHz, CDCl₃) δ 9.09 (d, J = 5.7 Hz, 8H), 8.90 (s, 8H), 8.19 (d, J = 5.7 Hz, 8H), -2.89 (s, 2H). MS (MALDI-MS) = 619.255 [M + H]⁺

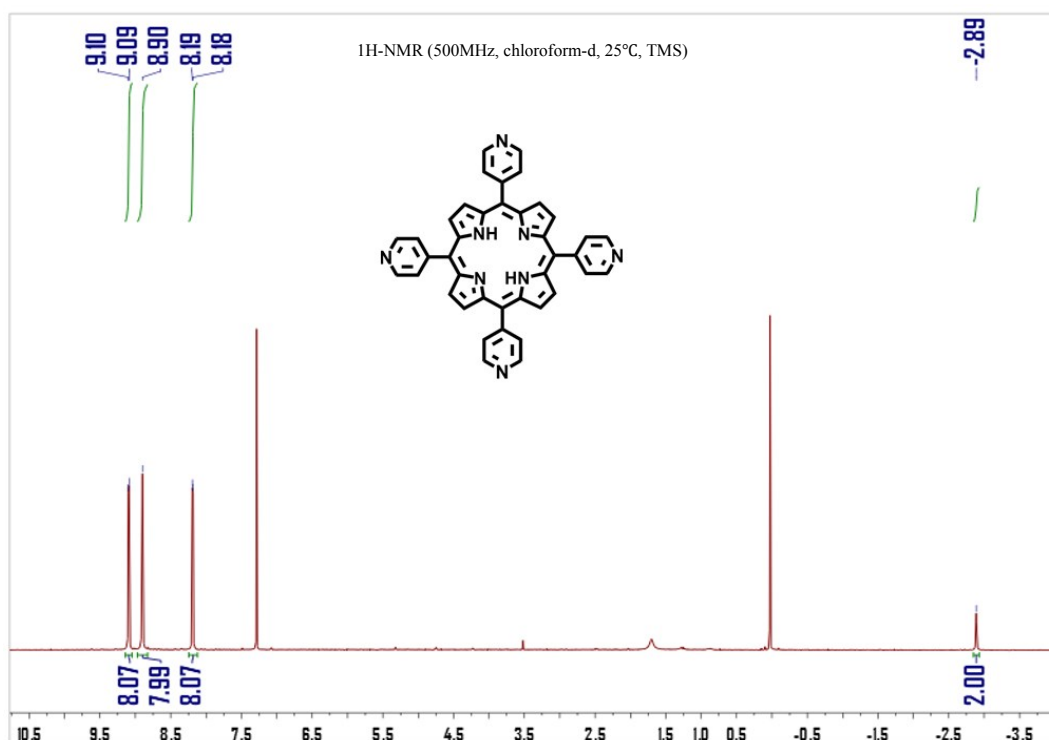


Figure S3: The ¹H-NMR (500MHz, chloroform-d, 25°C, TMS) spectrum of TPyP.

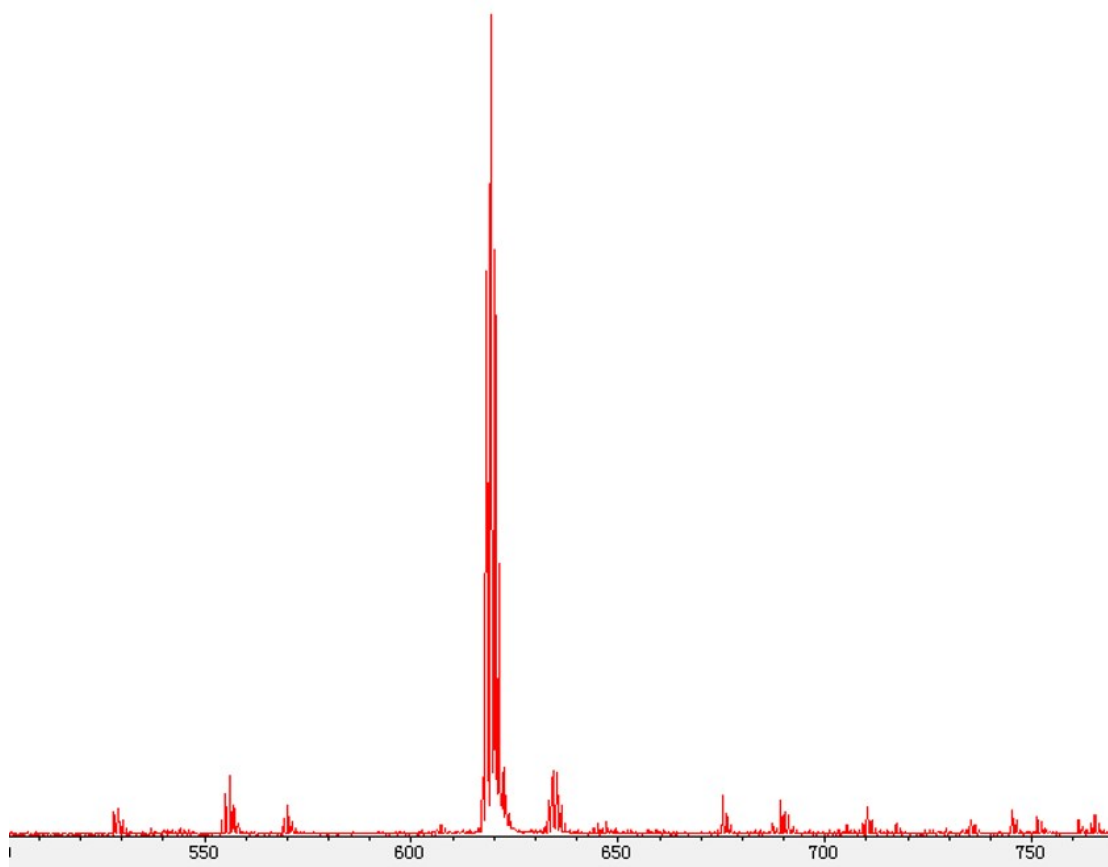


Figure S4: MALDI-TOF mass spectrometry analysis of TPyP.

Synthesis of 4,4',4'',4'''-(porphyrin-5,10,15,20-tetrayl) tetrakis (1-(6-carboxyhexyl) pyridin-1-ium) (CATPyP):

TPyP (200 mg, 0.32 mmol), 6-Bromohexanoic acid (2.52 g, 12.94 mmol), and 80 mL of N, N-Dimethylformamide were mixed together, then the mixture was heated to reflux under the condition of nitrogen atmosphere for 8 hours. After cooling to room temperature, the resulting precipitate was filtered and washed several times using trichloromethane, then dried under vacuum to obtain the dark red solid. ¹H NMR (500 MHz, DMSO) δ 12.16 (s, 4H), 9.62 (d, J = 6.3 Hz, 8H), 9.26 (s, 8H), 9.05 (d, J = 6.3 Hz, 8H), 4.99 (t, J = 7.0 Hz, 8H), 2.40 (t, J = 7.2 Hz, 8H), 2.35 – 2.28 (m, 8H), 1.79 – 1.73 (m, 8H), 1.67 – 1.60 (m, 8H), -3.08 (s, 2H). MS (ESI) = 1077.5 [M-3H-4Br]⁺.

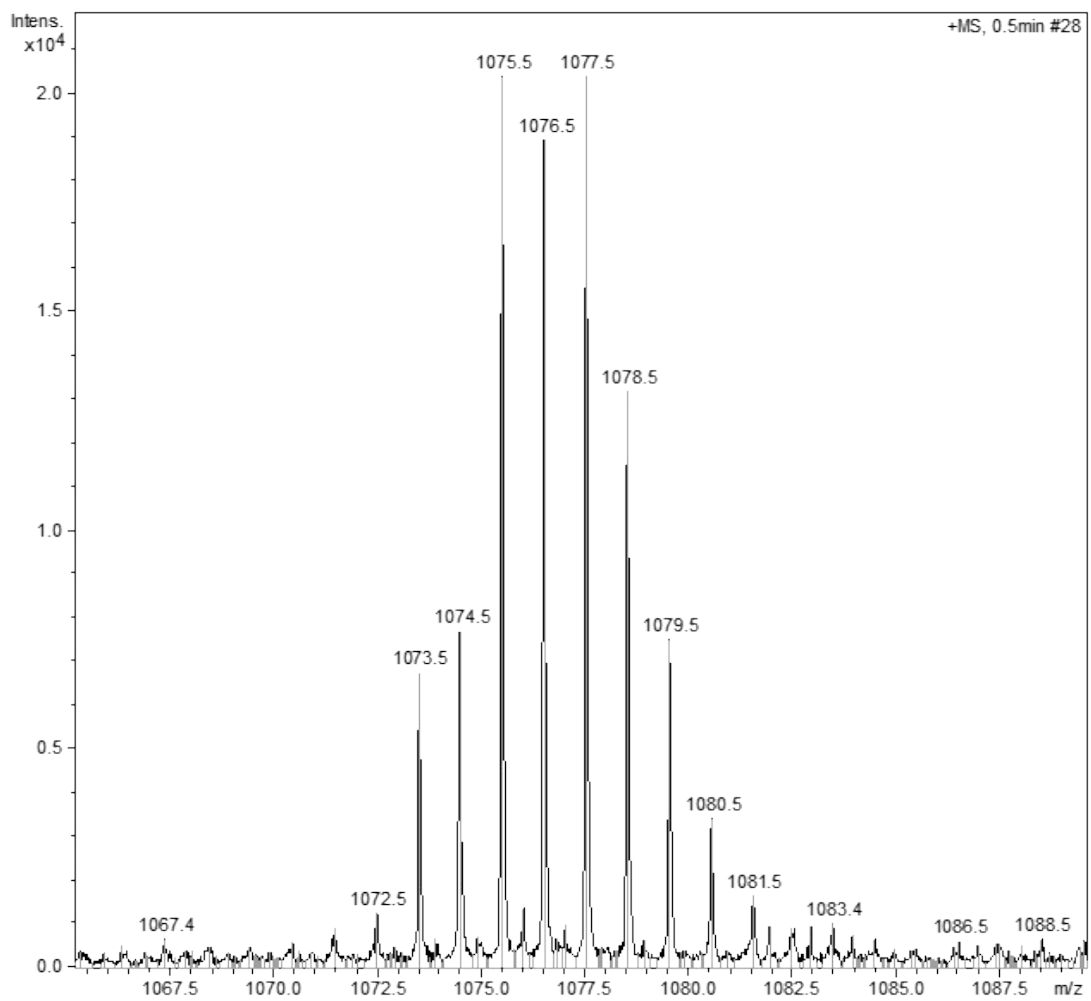
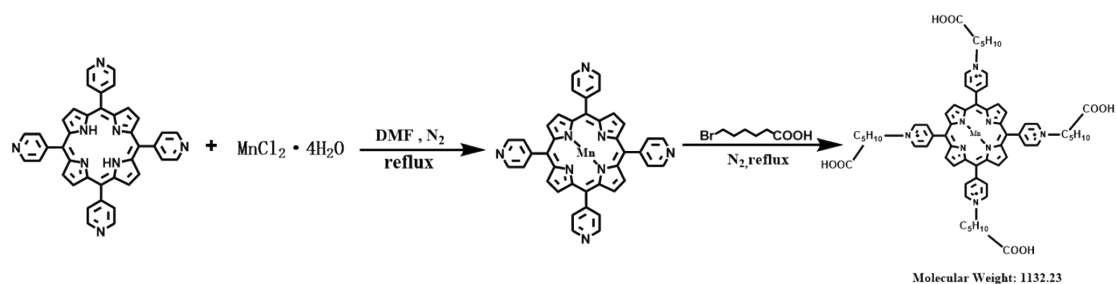


Figure S6: ESI-MS analysis of CATPyP.



Scheme S3: The synthetic route of Mn-TPyP and Mn-CATPyP.

Synthesis of 5, 10, 15, 20-tetrakis (4'-pyridyl) manganese (III) porphyrin (Mn-TPyP):

TPyP (500 mg, 0.81 mmol), $\text{MnCl}_2 \cdot 4\text{H}_2\text{O}$ (3.20g, 8.1mmol) and DMF (150 mL) were mixed together, then the mixture was heated to 80 °C under the condition of nitrogen atmosphere for 4 hours. After cooling to room temperature, the precipitate was filtered and washed several times using DMF. The crude product was purified by column chromatography and dried under vacuum to get the black product (69.54 mg, 0.095 mmol, 63%). MS (MALDI-MS) = 673.15. $[\text{M}+\text{H}]^+$

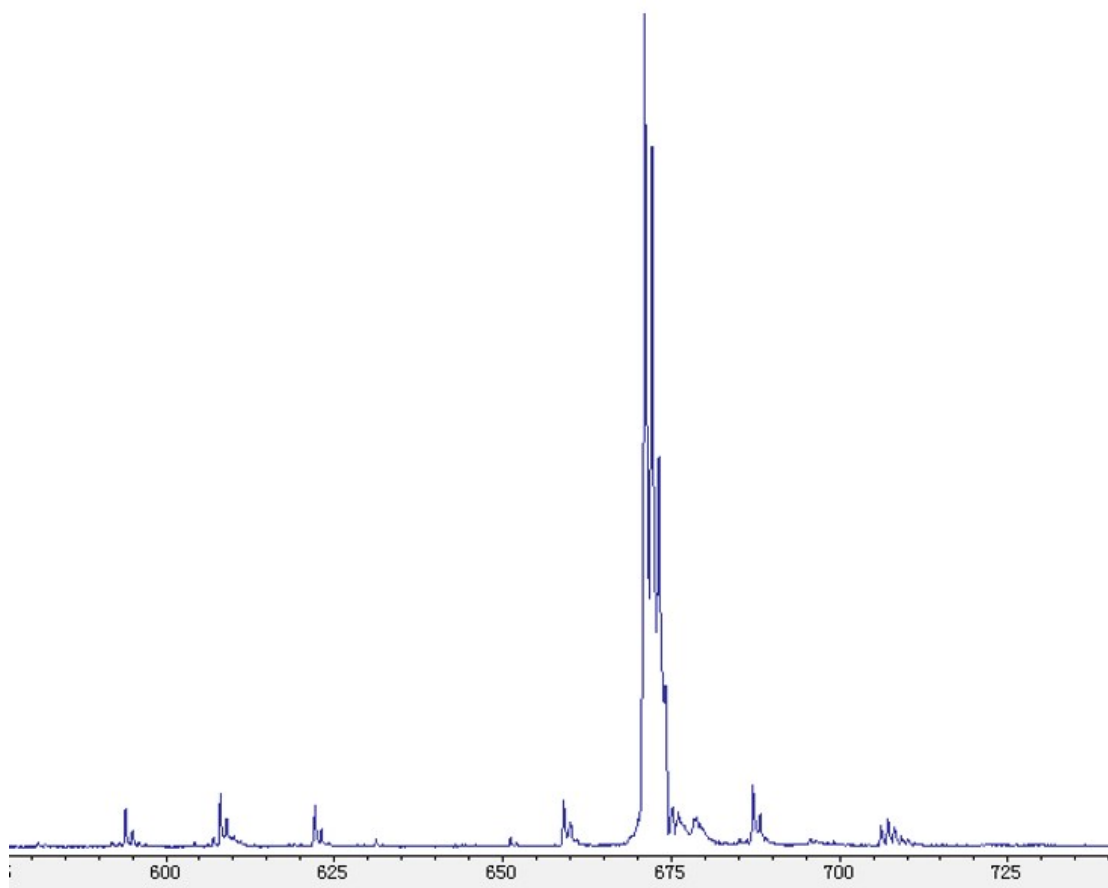


Figure S7: MALDI-TOF mass spectrometry analysis of Mn-TPyP.

Synthesis of 4,4',4'',4'''-(Mn (III) porphyrin-5,10,15,20-tetrayl) tetrakis (1-(6-carboxyhexyl) pyridin-1-ium) (Mn-CATPyP):

Mn-TPyP (200 mg, 0.29 mmol), 6-Bromohexanoic acid (2.32 g, 11.89 mmol), and 80 mL of N, N-Dimethylformamide were mixed together, then the mixture was heated to reflux under the condition of nitrogen atmosphere for 8 hours. After cooling to room temperature, the resulting precipitate was filtered and washed several times using trichloromethane, then dried under vacuum to obtain the dark red solid. MS (ESI) = 1129.4 [M-3H-4Br]⁺.

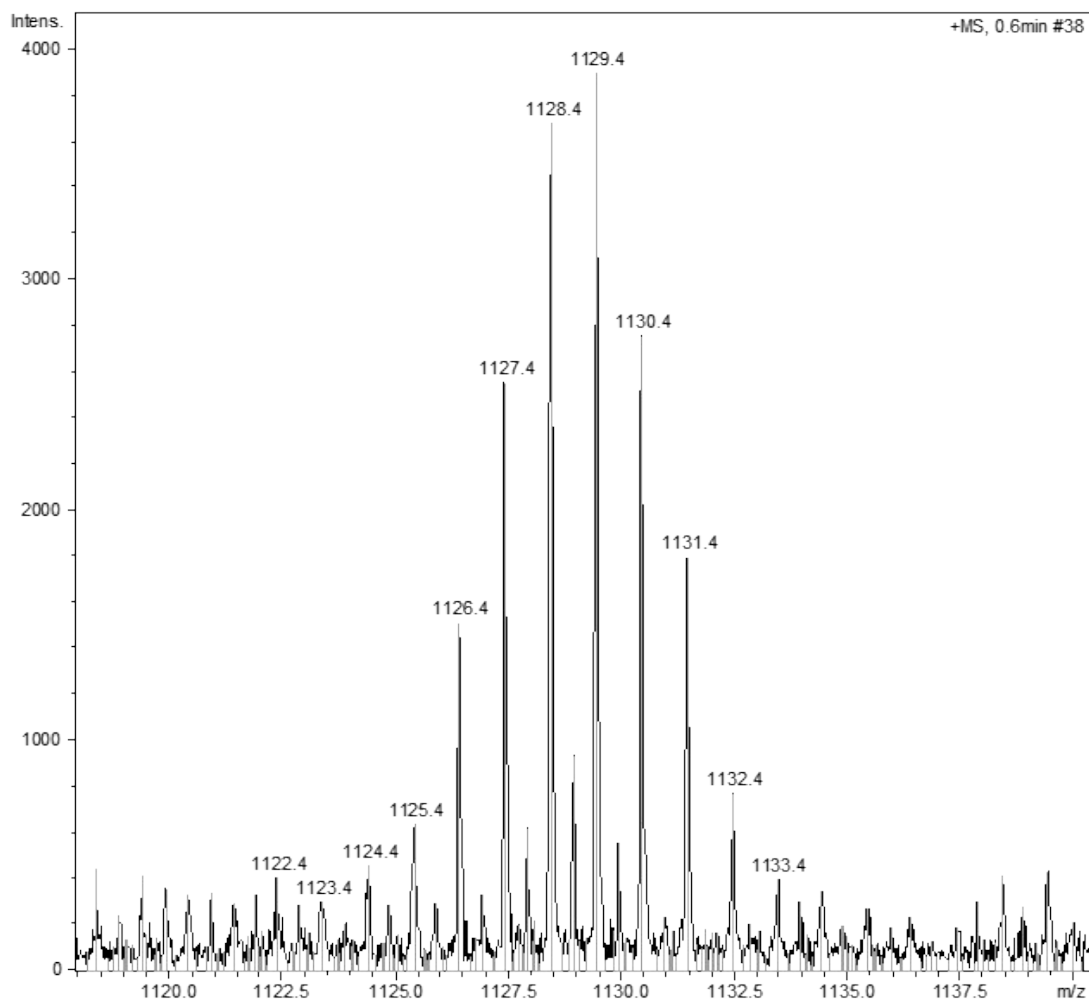


Figure S8: ESI-MS analysis of Mn-CATPyP.

2. Figures and table mentioned in manuscript

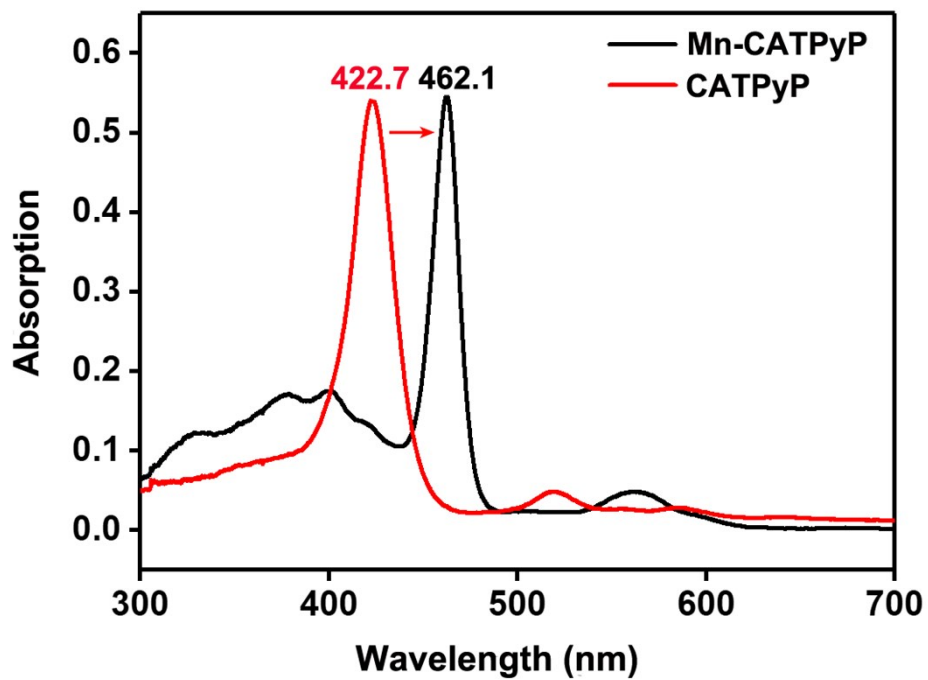


Figure S9: UV-vis absorption spectra of CATPyP and Mn-CATPyP.

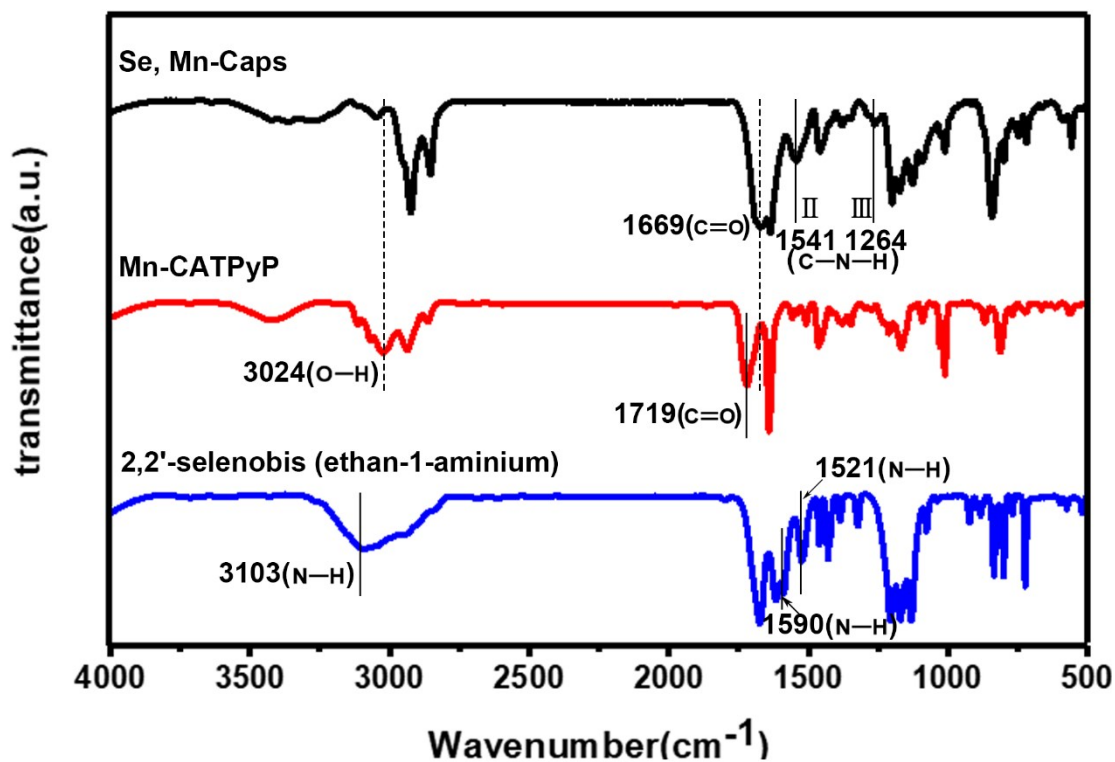


Figure S10: Fourier transform IR spectrum of Se, Mn-Caps (black line), Mn-CATPyP (red line), and 2, 2'-selenobis (ethan-1-aminium) (blue line).

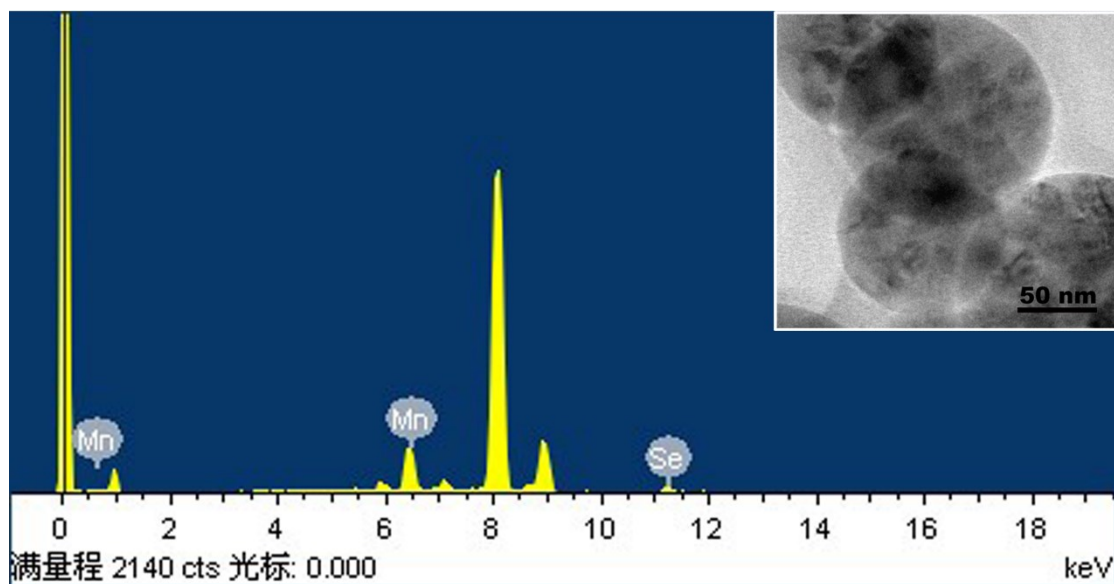


Figure S11: EDX analysis of the Se, Mn-Caps (insert: TEM image of Se, Mn-Caps).

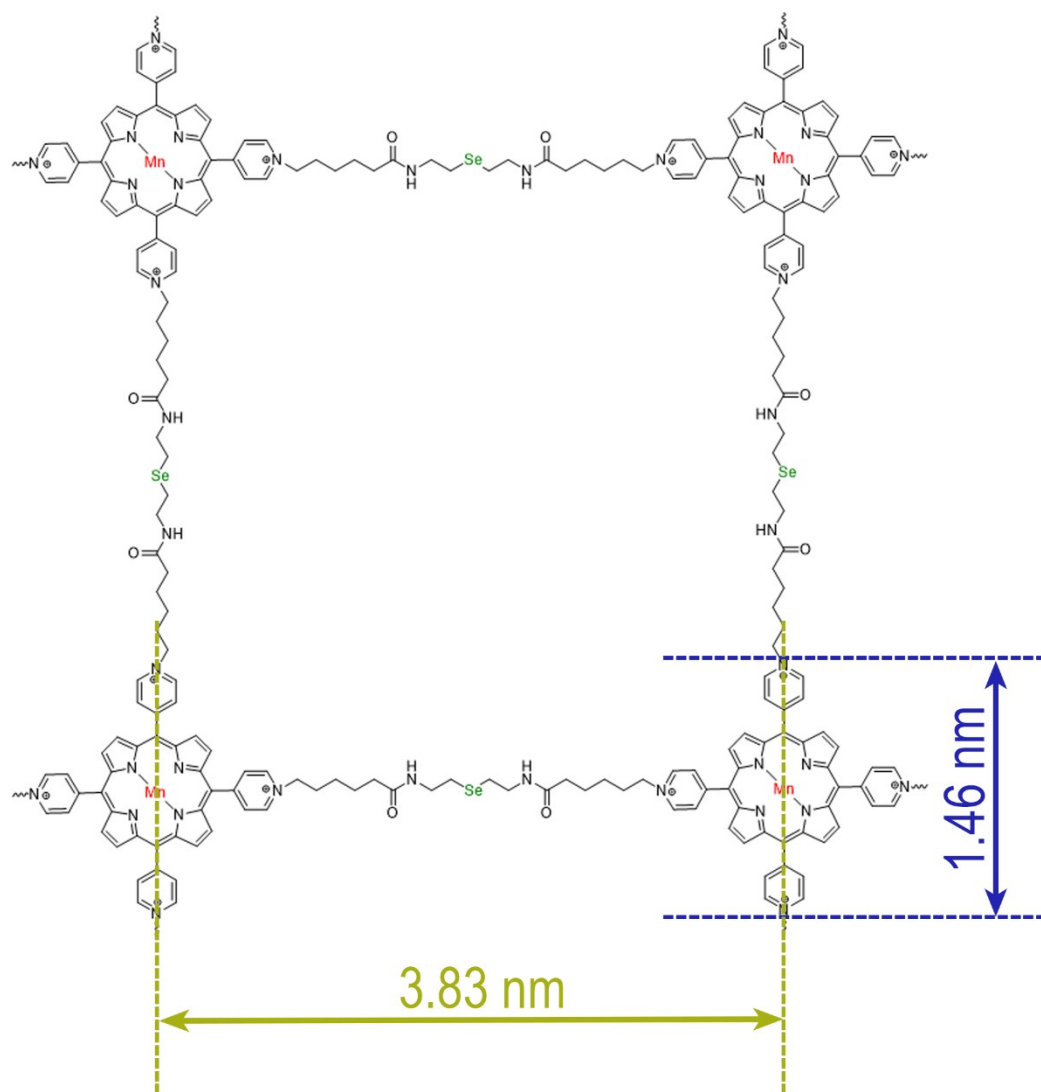


Figure. S12: The size of one Mn-TPyP molecule and the distance between two neighbouring Mn-CATPyP molecules for ordered arrangement bridged by 2,2'-selenobis (ethan-1-amine)

x

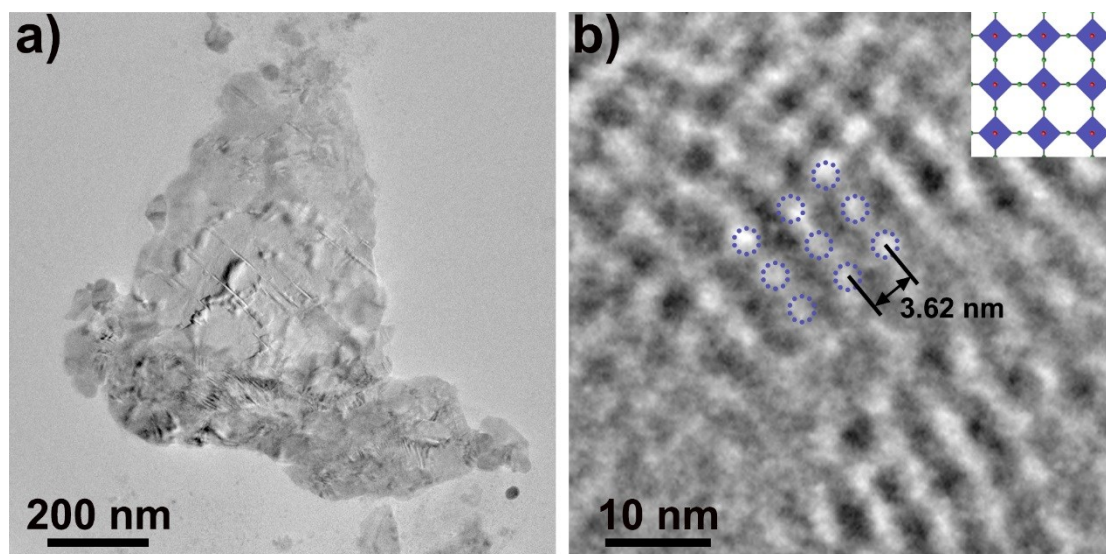


Figure S13 (a) HR-TEM image of the nanosheets formed when the polymerization proceeded for 4 hours. (b) Lattice-like structures observed from the nanosheets

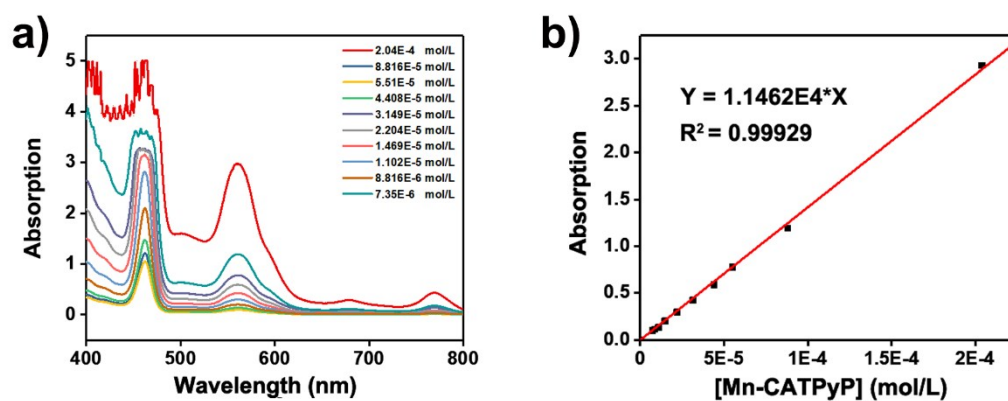


Figure S14: a) UV-vis absorption of Mn-CATPyP at different concentrations. b) a fitting curve between the UV absorption value and the concentration of Mn-CATPyP.

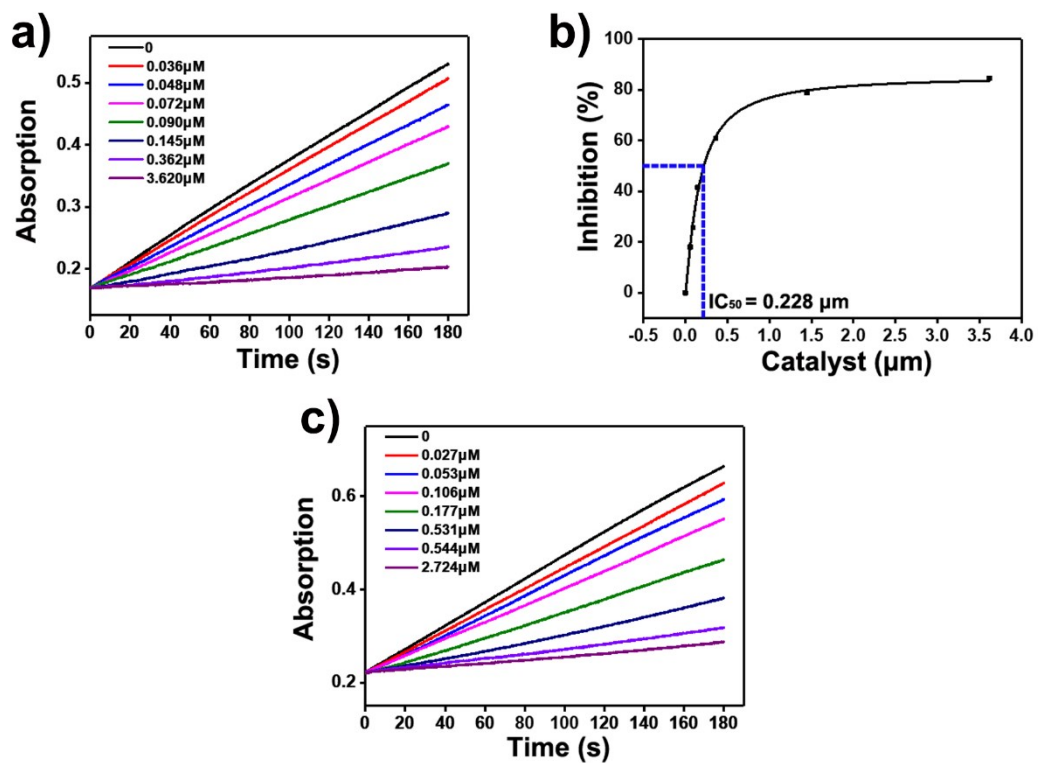


Figure S15: a) UV-vis absorption of blue methyl hydrazone at 560 nm and b) Percentage of inhibition of NBT oxidation by superoxide anion radical versus different concentrations of Mn-CATPyPs. c) UV-vis absorption of blue methyl hydrazone at 560 nm.

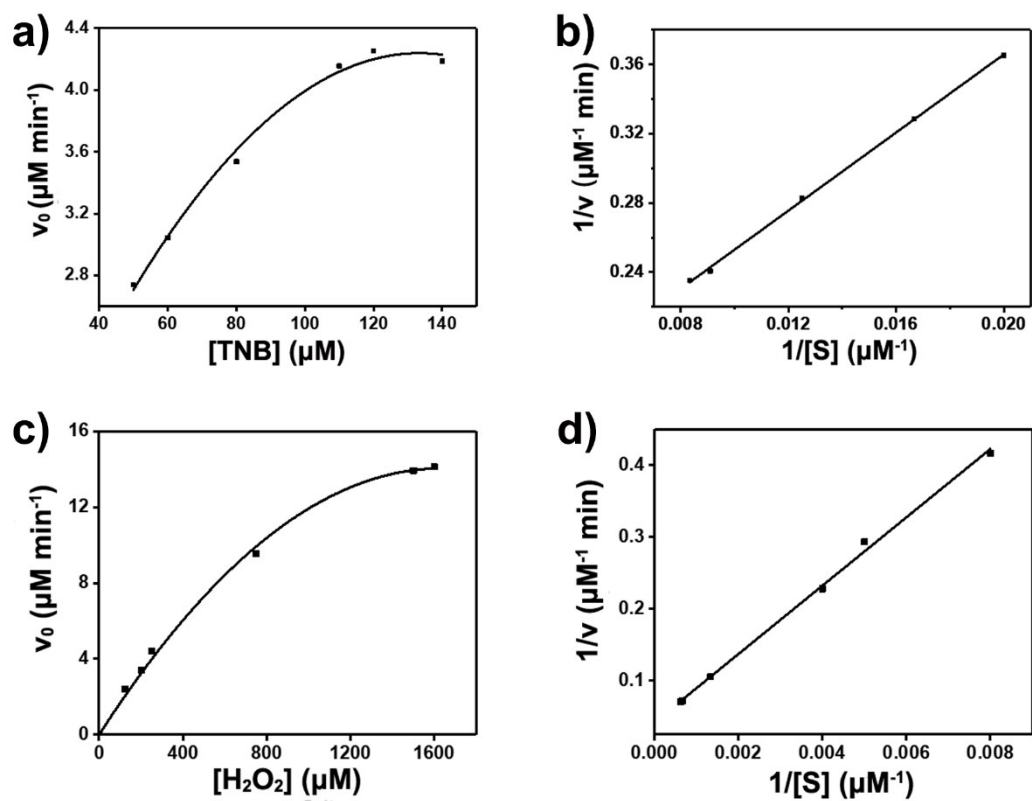


Figure S16: Steady-state kinetic assays of Se, Mn-Caps. (a) Michaelis–Menten and (b) Lineweaver-Burk plots for the TNB substrate (6.5 μM active site equivalent, 0.125 mM H_2O_2 , pH=7.0, TNB concentration was varied). (c) Michaelis–Menten and (d) Lineweaver–Burk plots for the H_2O_2 substrate (3.2 μM active site equivalent, 0.05 mM TNB, pH=7.0, H_2O_2 concentration was varied).

Table S1. Apparent Kinetic Parameters for H₂O₂ Reduction by TNB Catalyzed by Se, Mn-Caps

Substrate	k_{cat} (min ⁻¹)	K_{m} (mM)	$k_{\text{cat}}/K_{\text{m}}$ ($\times 10^4 \text{ M}^{-1} \text{ min}^{-1}$)
TNB	1.096 \pm 0.005	0.081 \pm 0.003	1.35 \pm 0.11
H ₂ O ₂	7.460 \pm 0.006	1.136 \pm 0.002	0.65 \pm 0.04

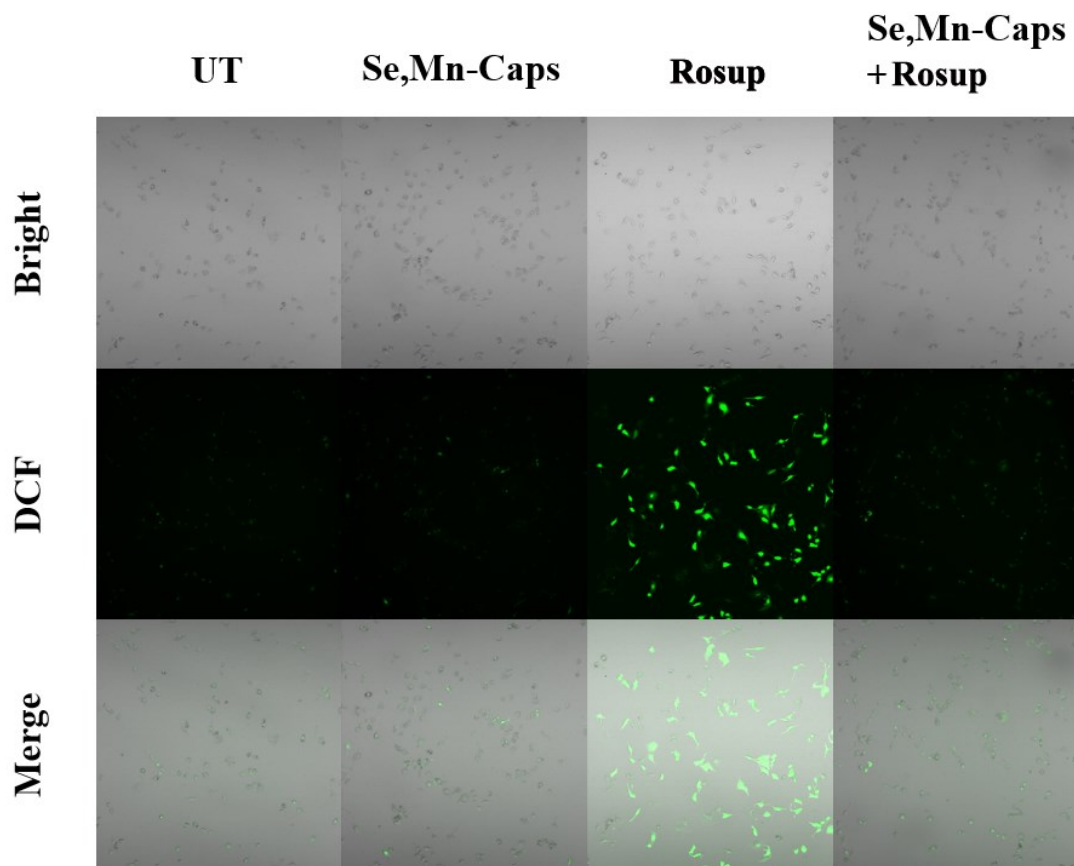


Figure S17: Fluorescence microscopy images of 3T3 cells with different treatments.

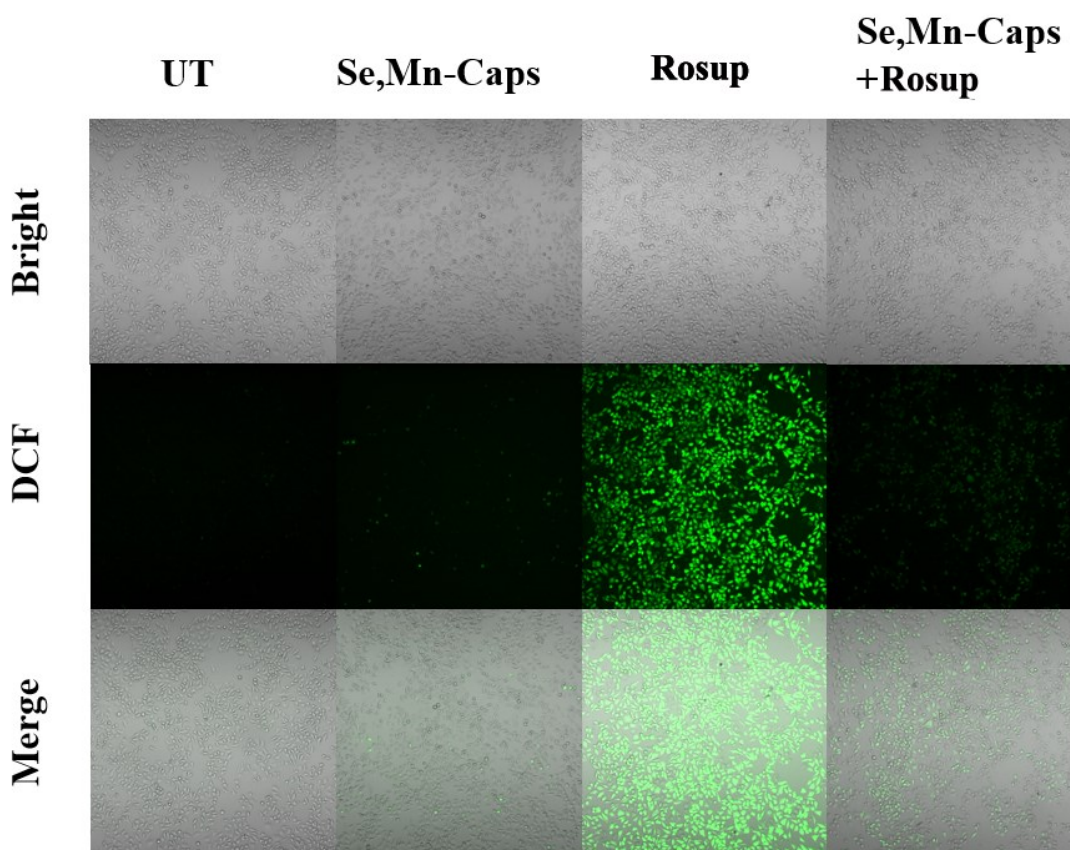


Figure S18: Fluorescence microscopy images of 3T3 cells with different treatments.

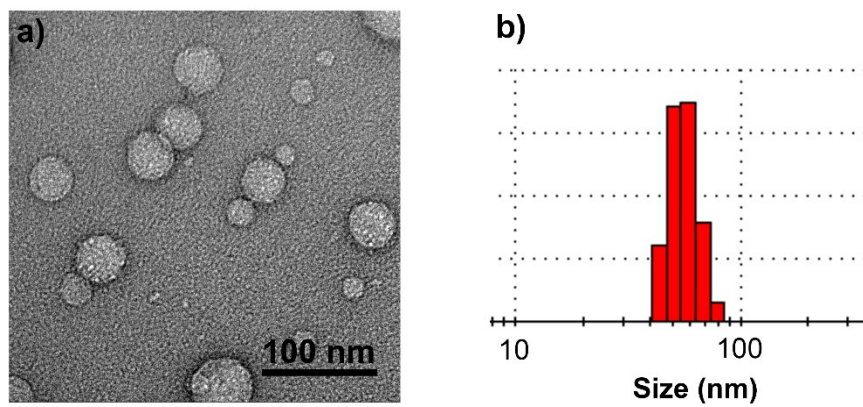


Figure S19: Image of covalently assembled caps without Se and Mn. (a) HR-TEM image. (b) DLS data of caps without Se and Mn (size distribution by number).